Hypoxia-Selective 3-Alkyl 1,2,4-Benzotriazine 1,4-Dioxides: The Influence of Hydrogen Bond Donors on Extravascular Transport and Antitumor Activity

Michael P. Hay,* Karin Pchalek,[†] Frederik B. Pruijn, Kevin O. Hicks, Bronwyn G. Siim,[‡] Robert F. Anderson, Sujata S. Shinde, Victoria Phillips,[#] William A. Denny, and William R. Wilson

Auckland Cancer Society Research Centre, Faculty of Medical and Health Sciences, The University of Auckland, Auckland, New Zealand

Tirapazamine (TPZ) and related 1,2,4-benzotriazine 1,4 dioxides (BTOs) are selectively toxic under hypoxia, but their ability to kill hypoxic cells in tumors is generally limited by their poor extravascular transport. Here we show that removing hydrogen bond donors by replacing the 3-NH₂ group of TPZ with simple alkyl groups increased their tissue diffusion coefficients as measured in multicellular layer cultures. This advantage was largely retained using solubilizing 3-alkylaminoalkyl substituents provided these were sufficiently lipophilic at pH 7.4. The high reduction potentials of such compounds resulted in rates of metabolism too high for optimal penetration into hypoxic tissue, but electron-donating 6- and 7-substituents moderated metabolism. Pharmacokinetic/pharmacodynamic model-guided screening was used to select BTOs with optimal extravascular transport and hypoxic cytotoxicity properties for evaluation against HT29 human tumor xenografts in combination with radiation. This identified four novel 3-alkyl BTOs providing greater clonogenic killing of hypoxic cells than TPZ at equivalent host toxicity, with the 6-morpholinopropyloxy-BTO **22** being 3-fold more active.

Introduction

Hypoxia has been demonstrated in a wide range of human tumors, and the prognostic significance of tumor hypoxia is becoming better understood.[1] In particular, hypoxia has a major role in driving progression, invasion, and metastasis,[2–6] as well as chemo-[7–9] and radioresistance.[10–12] Consequently, the search for agents that selectively target hypoxic tumor cells has become increasingly important.[9,13,14]

One approach to such selective targeting of hypoxic cells is exemplified by the hypoxic cytotoxin tirapazamine (TPZ,[a] **1**).[15,16] TPZ, a benzotriazine 1,4-dioxide (BTO), is a prodrug that undergoes selective bioreductive activation[17] under hypoxia to a DNA damaging species,[18,19] which may effect DNA strand breaks.[20–23] TPZ has been studied extensively in vitro and in vivo,[16,24] and in the clinic.[25] Despite indications of clinical activity, TPZ has a number of limitations that compromise its in vivo efficacy. In combination chemo-radiotherapy TPZ displays a range of significant toxicities that limit optimal delivery,[26–29] and its solubility is marginal. TPZ shows significantly reduced hypoxic selectivity in vivo (2- to 3-fold) compared to in vitro (hypoxic cytotoxicity ratio, HCR, ca. 50–100-fold).[30] This low hypoxic selectivity in tumors has been ascribed to rapid metabolism of TPZ in hypoxic tissues, leading to limited extravascular transport (EVT).[31–37] We have previously shown through modeling[32,38] and analogue studies[39,40] that improving EVT requires balancing the rate of bioreductive metabolism relative to the tissue diffusion of the analogues: analogues with low rates of bioreductive metabolism lack cytotoxic potency, while analogues with high rates of metabolism suffer poor EVT due to excessive consumption of the prodrug. Definition of the in vitro structure–activity relationships (SAR) between the one electron reduction potential, $E(1)$, and in vitro cytotoxicity for substituted BTO analogues allowed the rational design of BTO analogues with lowered electron affinity, derived from electron-donating substituents, which retain high hypoxic selectivity.[41] The analogues in that study were not designed to display increased aqueous solubility, and EVT was not explicitly considered. A later study of neutral BTOs demonstrated an increase in tissue diffusion coefficients, measured using multicellular layer (MCL) cultures, of analogues with increased lipophilicity.[39] Recently, we reported a systematic evaluation of 3-aminoalkylamino BTOs, seeking analogues with improved aqueous solubility and EVT.[40] This study showed that electron-donating substituents in the 6-position could be use to counteract increased rates of metabolism caused by the 3-aminoalkylamino substituents and demonstrated that sufficiently lipophilic analogues provide MCL penetration similar to TPZ and show activity against hypoxic cells in tumor xenografts. However, any improvements over TPZ were generally due to higher plasma concentrations at equivalent host toxicity, as in

---

* Corresponding author. Address: Auckland Cancer Society Research Centre, Faculty of Medical and Health Sciences, The University of Auckland, Private Bag 92019, Auckland 1142, New Zealand. Phone: 64-9-3737599 ext. 86598. Fax: 64-9-3737502. E-mail: m.hay@auckland.ac.nz.

† Current address: Boehringer Ingelheim Pharma GmbH & Co. KG, 55216 Ingelheim am Rhein, Germany.

‡ Current address: OXiGENE Inc., Magdalen Centre, Robert Robinson Avenue, The Oxford Science Park, Oxford OX4 4GA, United Kingdom.

Current address: Dept of Pharmacy and Pharmacology, University of Bath, Claverton Down, Bath BA2 7AY, United Kingdom.

[a] TPZ, tirapazamine; BTO, 1,2,4-benzotriazine-1,4-dioxide; HCR, hypoxic cytotoxicity ratio; EVT, extravascular transport; E(1), one-electron reduction potential; PK/PD, pharmacokinetic/pharmacodynamic; D, tissue diffusion coefficient; MCL, multicellular layer; k_{met}, first-order rate constant for bioreductive metabolism; SAR, structure activity relationships; MTD, maximum tolerated dose; $P_{7.4}$, octanol/water coefficient at pH 7.4; CT_{10}, area under concentration-time curve providing 10% surviving fraction; M_{10}, amount of BTO metabolized for 10% surviving fraction; $X_{1/2}$, calculated penetration half-distance into hypoxic tissue; SF, surviving fraction; LCK, log cell kill; AUC_{pred}, area under the plasma concentration−time curve required to give 1 log of cell of hypoxic cells in HT29 tumors; HCD, hypoxic cytotoxicity differential; LCK_{pred}, model-predicted logs of hypoxic cell kill.

the most active compound of this series (the 6-methoxy 3-aminoalkylamino BTO **2**), rather than increased EVT, which was generally no greater than for TPZ itself. There is thus potential for further improving therapeutic activity by increasing EVT of BTOs.
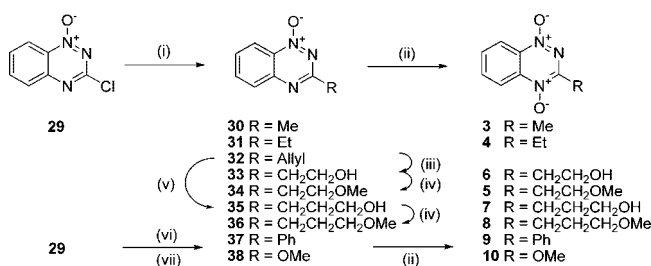
In this study, we test the hypothesis that removing hydrogen bond donors in the 3-position, by replacement of the 3-amino or 3-aminoalkyl groups with a 3-alkyl moiety, will provide a useful increase in EVT. Examples of 3-alkyl BTOs such as **3–5** have been examined previously,[42] and although some (e.g., **4**, **5**) were active in vivo they were not superior to TPZ. However, replacement of the strongly electron donating amine with the weaker alkyl substituent raises the reduction potential; we therefore hypothesized that the rates of bioreductive metabolism of such compounds may be too high for adequate EVT. Thus, in the present study we sought to apply the strategies developed previously to optimize 3-aminoalkyl analogues,[40] particularly the use of electron-donating substituents in the 6- or 7-position to counteract high rates of metabolism expected to be conferred by 3-alkylaminoalkyl side chains.

Maximizing activity against hypoxic cells in tumors requires optimizing all aspects of drug action, including cytotoxic potency and plasma pharmacokinetics, not just EVT. To integrate all such elements, as in the previous study,[40] we have used a spatially resolved pharmacokinetic/pharmacodynamic (PK/PD) model to guide identification of synthetic targets and selection of priority compounds for in vivo evaluation. We have previously validated this model by demonstrating its ability to predict killing of hypoxic cells in HT29[37] and SiHa tumors.[38] This mathematical model uses EVT parameters measured in vitro (tissue diffusion coefficient, D, determined in aerobic MCLs, and the first-order rate constant for bioreductive metabolism in hypoxic cell suspensions, k_{met}) to calculate the drug concentration−time profile at each position in a tumor microvascular network, using the measured plasma PK as input. The model then applies the PK/PD (exposure/cell killing) relationship determined in vitro to calculate the probability of cell kill at each position within the tumor region defined by the microvascular network, and the overall drug-induced kill in the hypoxic subpopulation. Here we apply this approach to a series of 3-alkyl BTOs **3–28** with solubilizing alkylamine side chains, linked at either the 3-position or through electron-donating alkoxy linkers at the 6- and 7-positions. This approach efficiently identified four new 3-alkyl BTOs with in vivo activity against hypoxic tumor cells as well as confirming the activity of the known BTO analogues **4** and **5**.
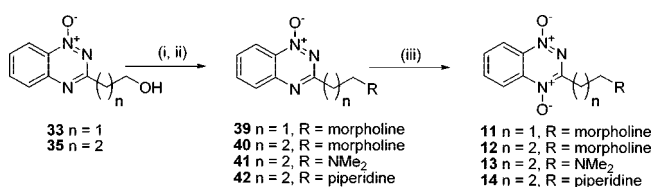
Chemistry

Synthesis. We have previously demonstrated an efficient synthetic approach to the known BTO analogues **4** and **5** using a Stille coupling to install the 3-alkyl substituent into a BTO 1-oxide.[43] This represented a significant improvement on the Bamberger approach previously used to generate the 3-alkyl-BTO 1-oxide.[42] We extended this methodology to 6- and 7-substituted (F, Me, MeO) BTOs and further increased the efficiency of the Stille coupling through application of microwave reaction conditions.[44] Thus, 3-chloride **29**[44] underwent Stille coupling with various stannanes and Pd(PPh$_3$)$_4$ to give 3-alkyl 1-oxides **30–32** (method A, Scheme 1). Ozonolysis of the allyl side chain of **32** followed by a reductive workup gave the ethanol **33**, which was alkylated to give ether **34**. Hydroboration of alkene **32** gave the propanol **35**, which was also alkylated to give ether **36**. Suzuki coupling of chloride **29** gave the 3-phenyl BTO **37**, while nucleophilic substitution of **29** with
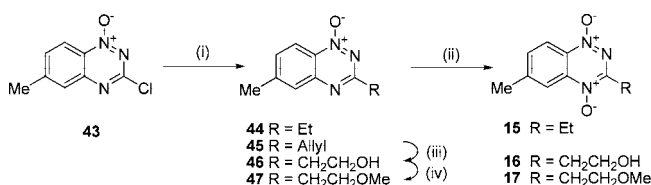
Scheme 1[a]

30 R = Me
31 R = Et
32 R = Allyl
33 R = CH$_2$CH$_2$OH
34 R = CH$_2$CH$_2$OMe
35 R = CH$_2$CH$_2$CH$_2$OH
36 R = CH$_2$CH$_2$CH$_2$OMe
37 R = Ph
38 R = OMe

3 R = Me
4 R = Et
6 R = CH$_2$CH$_2$OH
5 R = CH$_2$CH$_2$OMe
7 R = CH$_2$CH$_2$CH$_2$OH
8 R = CH$_2$CH$_2$CH$_2$OMe
9 R = Ph
10 R = OMe

[a] Reagents: (i) Pd(PPh$_3$)$_4$, stannane, DME, reflux (method A); (ii) CF$_3$CO$_3$H, DCM (method B); (iii) O$_3$, MeOH/DCM, −78 °C; NaBH$_4$, EtOH, −40 °C; (iv) TMSCH$_2$N$_2$, HBF$_4$, DCM; (v) 9-BBN, THF; NaOH, H$_2$O$_2$, (vi) Pd(PPh$_3$)$_4$, PhB(OH)$_2$, Cs$_2$CO$_3$, H$_2$O, DME, reflux; (vii) NaOMe, MeOH.

Scheme 2[a]

33 n = 1
35 n = 2

39 n = 1, R = morpholine
40 n = 2, R = morpholine
41 n = 2, R = NMe$_2$
42 n = 2, R = piperidine

11 n = 1, R = morpholine
12 n = 2, R = morpholine
13 n = 2, R = NMe$_2$
14 n = 2, R = piperidine

[a] Reagents: (i) MsCl, Et$_3$N, DCM; (ii) amine (method C); (iii) CF$_3$CO$_3$H, CF$_3$CO$_2$H, DCM (method B).

Scheme 3[a]

44 R = Et
45 R = Allyl
46 R = CH$_2$CH$_2$OH
47 R = CH$_2$CH$_2$OMe

15 R = Et
16 R = CH$_2$CH$_2$OH
17 R = CH$_2$CH$_2$OMe

[a] Reagents: (i) Pd(PPh$_3$)$_4$, stannane, DME, reflux (method A); (ii) CF$_3$CO$_3$H, DCM (method B); (iii) O$_3$, MeOH/DCM, −78 °C; NaBH$_4$, EtOH, −40 °C; (iv) TMSCH$_2$N$_2$, HBF$_4$, DCM.

methoxide gave the 3-alkoxy BTO **38**. The BTO 1-oxides **30**, **31**, and **33–38** were oxidized to the corresponding 1,4-dioxides **3–10** using trifluoroperacetic acid in DCM (method B). The alcohols **33** and **35** were elaborated to alkylamines **39–42** via the corresponding mesylates with displacement by the appropriate amines (method C, Scheme 2). Selective aromatic N-oxidation of the 1-oxides **39–42** was achieved using trifluoroperacetic acid in the presence of trifluoroacetic acid to protect the amine side chain as the salt and gave modest yields of **11–14** (method B). It was not possible to prepare C2 homologues of the C3 BTOs **13** and **14** because of the instability of the products under the reaction conditions. Attempts to convert the corresponding dioxide alcohol **6** to these analogues via mesylation and displacement with either dimethylamine or piperidine were unsuccessful with loss of the 4-oxide being observed.

Stille coupling of the 6-methyl BTO 3-chloride **43**[44] with the appropriate stannane gave the 3-ethyl BTO 1-oxide **44** and the 3-allyl-BTO 1-oxide **45** (method A, Scheme 3). Ozonolysis of **45** gave ethanol **46**, which was alkylated to give ether **47**. Oxidation of **44**, **46**, and **47** with trifluoroperacetic acid gave the corresponding 1,4-dioxides **15–17**. Nucleophilic displacement of the fluorides **48** and **49** with various alkoxides gave 6-alkoxy BTO 1-oxides **50–56** and 7-alkoxy BTO 1-oxides **57–59**, respectively (method D, Scheme 4). Oxidation with trifluoroperacetic acid, using trifluoroacetic acid protection of the amine side chain, where appropriate, gave the BTO 1,4-

Scheme 4[a]
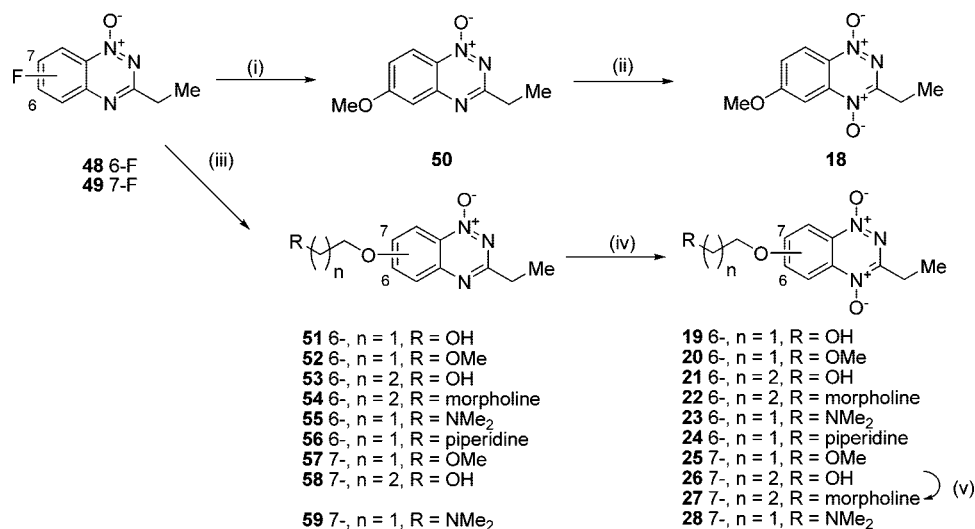
[a] Reagents: (i) NaOMe, MeOH; (ii) CF₃CO₃H, DCM (method B); (iii) NaH, alcohol, THF, or DMF (method D); (iv) CF₃CO₃H, CF₃CO₂H, DCM (method B); (v) MsCl, Et₃N, DCM; morpholine (method C).
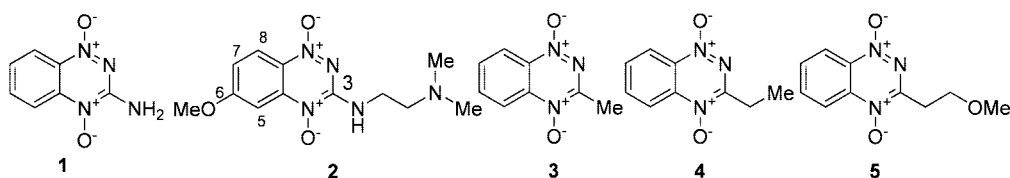

Figure 1

dioxides **18–26**, and **28** (method B). Morpholide **27** was prepared from the alcohol **26** via the mesylate.

Physicochemical Measurements. Solubilities of the BTOs **3–28** were determined in culture medium containing 5% fetal calf serum, at 22 °C. Octanol/water partition coefficients were measured at pH 7.4 ($P_{7.4}$) for TPZ, **3** and a subset of six BTOs by a low volume shake flask method, with BTO concentrations in both the octanol and the buffer phases analyzed by HPLC as previously described.[40,45] These values were used to "train" ACD LogP/LogD prediction software (v. 8.0, Advanced Chemistry Development Inc., Toronto, Canada) using a combination of ACD/LogP System Training and Accuracy Extender. Apparent (macroscopic) pK_a values for the side chain were calculated using ACD pK_a prediction software (v. 8.0, Advanced Chemistry Development Inc., Toronto, Canada).

One Electron Reduction Potential Measurements $E(1)$. Pulse radiolysis experiments were performed on The University of Auckland Dynaray 4 (4 MeV) linear accelerator (200 ns pulse length with a custom-built optical radical detection system). $E(1)$ values for the compounds were determined in anaerobic aqueous solutions containing 2-propanol (0.1 M) buffered at pH 7.0 (10 mM phosphate) by measuring the equilibrium constant[46] for the electron transfer between the radical anions of the compounds and the appropriate viologen or quinone reference standard. Data were obtained at three concentration ratios at room temperature (22 ± 2 °C) and used to calculate the ΔE between the compounds and references, allowing for ionic strength effects on the equilibria.

Biological Methods

In vitro Assays. A schematic of the testing algorithm, guided by the spatially resolved PK/PD model, is shown in Figure 2.

Cytotoxic potency was determined by IC₅₀ assays, using 4 h drug exposure of HT29 and SiHa cells under aerobic and anoxic
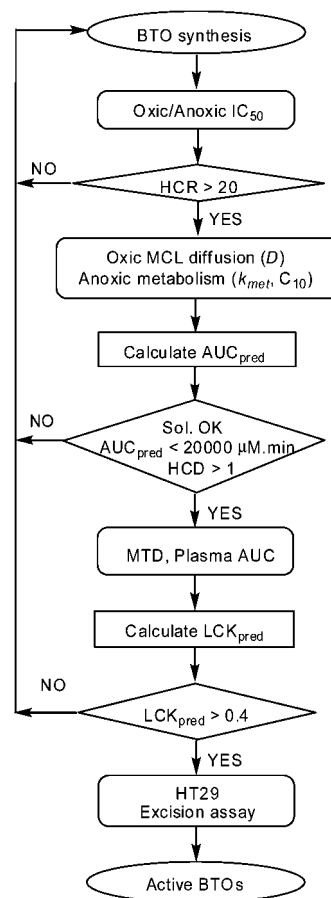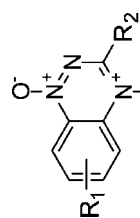

Figure 2. Flowchart of PK/PD model guided drug evaluation of BTOs.

Table 1. Physicochemical, In Vitro, and Modeling Parameters for **1** and BTOs **3–14**
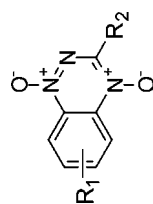

3-14

no.	R_1	R_2	pK_a[a]	$\log P_{7,4}$ calc[b]	sol[c] mM	HT29 IC_{50} hypox μM	HT29 HCR[d]	SiHa IC_{50} hypox μM	SiHa HCR[d]	D_{calc}[e,f]	$E(1)$ mV	k_{met}[f,g] min^{-1}	$X_{1/2}$[f,h] μm	PK/PD model	CT_{10}[i] μM	AUC_{pred}[j] μM·min	HCD[k]
1[l]	H	NH$_2$	na[m]	−0.33	9	5.1	71	2.5	107	4.2	−456	0.58	45	C × M	24.3	10300	4.1
3	H	−CH$_3$	na[m]	−0.23	28	4.1	67	3.0	57	25.9	−364	4.87	34	M	25.3	47100	6.0
4	H	−CH$_2$CH$_3$	na[m]	0.34	15	6.8	54	5.9	84	28.3	−376	1.90	63	M	19.7	7450	8.2
5	H	−(CH$_2$)$_2$OCH$_3$	na[m]	−0.26	>21	3.5	49	1.6	61	19.2	−353	2.00	55	M	21.3	5400	6.2
6	H	−(CH$_2$)$_2$OH	na[m]	−0.91	34	3.7	153	1.7	526	5.1	−360	2.89	21	M	18.1	165000	1.3
7	H	−(CH$_2$)$_3$OH	na[m]	−0.47	50	3.7	110	3.1	85	7.3	−364	1.94	27	M	30.2	33000	0.9
8	H	−(CH$_2$)$_3$OCH$_3$	na[m]	−0.02	21	6.9	86	2.4	272	21.0		3.78	40	M	26.7	30100	7.3
9	H	−C$_6$H$_4$	na[m]	1.46	0.3	4.4	2	2.2	1	27.8	−352						
10	H	−OCH$_3$	na[m]	−0.30	23	3.1	1	1.1	4	20.1							
11	H	−(CH$_2$)$_2$NMORPH	6.04	−0.45	42	3.8	107	2.2	225	11.6		4.20	28	M	10.0	38900	1.2
12	H	−(CH$_2$)$_3$NMORPH	7.07	−1.45	>46	2.2	91	1.0	132	4.5		5.52	20	M	3.2		
13	H	−(CH$_2$)$_3$N(CH$_3$)$_2$	8.89	−1.37	51	0.39	71	0.2	58	7.3	−327	6.78	18	M	2.1	80600	0.3
14	H	−(CH$_2$)$_3$NPIP	9.05	−1.27	43	1.0	36	0.6	55	7.5		6.66	17	M	1.5	92000	0.3

[a] Calculated using ACD pK_a. [b] Calculated using ACD logD. [c] Solubility in culture medium. [d] Hypoxia cytotoxicity ratio = oxic IC_{50}/hypoxic IC_{50}. [e] Diffusion coefficient in HT29 MCLs × 10^{-7} cm^2 s^{-1}. [f] Error estimates are provided in the Supporting Information. [g] First-order rate constant for metabolism in anoxic HT29 cell suspensions, scaled to the cell density in MCLs. [h] Penetration half-distance in anoxic HT29 tumor tissue (see text). [i] Area under the concentration–time curve providing 10% surviving fraction in the clonogenic assay. [j] Predicted area under the plasma concentration–time curve required to give 1 log of cell kill in addition to that produced by a single 20 Gy dose of γ radiation. [k] In vivo hypoxic cytotoxicity differential = LCK$_{hypoxic}$/LCK$_{oxic}$. [l] Data from ref 40. [m] Not applicable.

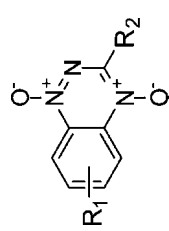**Table 2.** Physicochemical, in Vitro, and Modeling Parameters for BTOs **1**, **2**, and **15–28**

15-28

no.	R_1	R_2	pK_a [a]	$logP_{7,4}$ calc[b]	sol[c] mM	HT29 IC$_{50}$ hypox μM	HT29 HCR[d]	SiHa IC$_{50}$ hypox μM	SiHa HCR[d]	D_{calc}[e,f]	E(1) mV	k_{met}[f,g] min^{-1}	$X_{½}$[f,h] μm	PK/PD model	CT$_{10}$[i] μM	AUC$_{pred}$[j] μM·min	HCD[k]
1[l]	H	–NH$_2$	na[m]	−0.33	9	5.1	71	2.5	107	4.2	−456	0.58	45	C × M	24.3	10300	4.1
2[l]	6-CH$_3$O–	NH(CH$_2$)$_2$NMe$_2$	8.47	−0.85	46	7.7	89	2.9	232	2.9	−500	0.54	35	C × M	26.1	13800	2.7
15	6-CH$_3$–	–CH$_2$CH$_3$	na[m]	0.70	4	11.4	63	3.6	214	28.6	−418	0.66	112	C × M	52.4	8970	8.1
16	6-CH$_3$–	–(CH$_2$)$_2$OH	na[m]	−0.45	7	4.3	82	1.2	208	7.4		0.82	51	C × M	22.2	8430	4.7
17	6-CH$_3$–	–(CH$_2$)$_2$OCH$_3$	na[m]	0.20	3	6.6	63	1.9	150	22.7		0.93	73	M	57.9	8130	7.1
18	6-CH$_3$O–	–CH$_2$CH$_3$	na[m]	0.43	3	16.8	73	6.8	175	25.0	−472	0.30	156	C × M	69.9	8720	10.8
19	6-HO(CH$_2$)$_2$O–	–CH$_2$CH$_3$	na[m]	−0.55	21	14.4	54	7.9	203	4.5		0.15	94	C × M	97.3	13200	9.1
20	6-CH$_3$O(CH$_2$)$_2$O–	–CH$_2$CH$_3$	na[m]	0.09	3	17.9	120	14.2	70	17.4		0.23	148	M^2	213.2	14000	10.5
21	6-HO(CH$_2$)$_3$O–	–CH$_2$CH$_3$	na[m]	0.23	10	17.0	54	8.6	105	9.1		0.13	140	C × M	108.9	13000	10.5
22	6-MORPHN(CH$_2$)$_3$O–	–CH$_2$CH$_3$	7.28	0.13	>47	6.8	153	4.3	217	12.4	−440	0.53	64	C × M	38.6	7600	6.5
23	6-(CH$_3$)$_2$N(CH$_2$)$_2$O–	–CH$_2$CH$_3$	8.15	−0.53	>49	1.3	307	0.8	374	10.7		1.79	42	C × M	5.1	3630	1.9
24	6-PIPN(CH$_2$)$_2$O–	–CH$_2$CH$_3$	8.31	0.48	>48	1.5	254	1.0	302	19.0		1.22	67	M	6.8	1980	5.9
25	7-CH$_3$O(CH$_2$)$_2$O–	–CH$_2$CH$_3$	na[m]	−0.27	2	4.7	69	1.8	116	13.7		0.49	90	C × M	40.7	5660	8.3
26	7-HO(CH$_2$)$_3$O–	–CH$_2$CH$_3$	na[m]	−0.13	17	6.9	146	2.7	161	6.4		0.44	65	C × M	31.6	6330	6.0
27	7-MORPHN(CH$_2$)$_3$O–	–CH$_2$CH$_3$	7.29	−0.24	>48	3.0	147	1.3	181	9.1	−396	0.73	60	M	7.1	3090	6.0
28	7-(CH$_3$)$_2$N(CH$_2$)$_2$O–	–CH$_2$CH$_3$	8.16	−0.90	>51	0.7	105	0.5	128	7.6		3.14	26	M	1.8	1250	3.6

[a] Calculated using ACD pK_a. [b] Calculated using ACD logD. [c] Solubility in culture medium. [d] Hypoxia cytotoxicity ratio = oxic IC$_{50}$/hypoxic IC$_{50}$. [e] Diffusion coefficient in HT29 MCLs × 10^{-7} cm^2 s^{-1}. [f] Error estimates are provided in the Supporting Information. [g] First-order rate constant for metabolism in anoxic HT29 cell suspensions, scaled to the cell density in MCLs. [h] Penetration half-distance in anoxic HT29 tumor tissue (see text). [i] Area under the concentration–time curve providing 10% surviving fraction in the clonogenic assay. [j] Predicted area under the plasma concentration–time curve required to give 1 log of cell kill in addition to that produced by a single 20 Gy dose of γ radiation. [k] In vivo hypoxic cytotoxicity differential = LCK$_{hypoxic}$/LCK$_{oxic}$. [l] Data from ref 40. [m] Not applicable.

Table 3. In Vivo Parameters for Selected BTOs

no.	R_1	R_2	AUC_{pred}^{b} μM·min	HCD^{c}	$form^{d}$	MTD^{e} μmol kg⁻¹	$dose^{f}$ μmol kg⁻¹	plasma pharmacokinetics C_{max} (μM)	$t_{1/2}$ (min)	AUC μM·min	drug only[g] mean	SEM	p	RT + drug[h] pred[i]	mean	SEM	p
1[j]	H	NH_2	10300	4.1	A	178	133	61.7	36.3	2950	0.15	0.08	ns[k]	0.31	0.59	0.15	<0.01
2[j]	6-CH_3O-	$-NH(CH_2)_2N(CH_3)_2$	13800	2.7	B	1000	1000	157.0	51.5	14400	0.15	0.04	0.04	1.60	1.84	0.16	<0.01
4	H	$-CH_2CH_3$	7450	8.2	C	562	562	271.1	11.2	8780	0.11	0.03	ns[k]	1.12	0.89	0.13	<0.01
5	H	$-(CH_2)_2OCH_3$	5400	6.2	C	421	421	175.8	18.0	6780	0.30	0.01	ns[k]	0.89	0.80	0.15	<0.05
18	6-CH_3O-	$-CH_2CH_3$	8720	10.8	D	750	562	71.5		8310				0.41	0.76	0.18	<0.05
22	6-MORPHN$(CH_2)_3O-$	$-CH_2CH_3$	7600	6.5	A	1000	750	149.6	34.8	9740	0.14	0.02	ns[k]	1.82	1.66	0.17	<0.001
23	6-$(CH_3)_2N(CH_2)_2O-$	$-CH_2CH_3$	3630	1.9	A	562	421	55.5	32.2	3340	0.23	0.11	0.08	2.05	0.88	0.26	<0.001
24	6-PIPN$(CH_2)_2O-$	$-CH_2CH_3$	1980	5.9	A	178	133	9.8	25.0	465				0.10			
27	7-MORPHN$(CH_2)_3O-$	$-CH_2CH_3$	3090	6.0	A	421	316	30.1	36.0	1980				0.87	0.98	0.13	<0.05

[a] Penetration half-distance in anoxic HT29 tumor tissue (see text). [b] Predicted area under the plasma concentration–time curve required to give 1 log of cell kill in addition to that produced by a single 20 Gy dose of γ radiation. [c] In vivo hypoxic cytotoxicity differential = LCK$_{hypoxic}$/LCK$_{oxic}$. [d] Formulation: A, 0.9% saline; B, pH 4, 0.1 M sodium lactate buffer; C, 5% DMSO/saline; D, 10% DMSO/40% PEG-400/saline. [e] Maximum tolerated single i.p. dose. [f] Dose given for pharmacokinetic and activity assays. [g] Compared to unirradiated controls treated with vehicle only. [h] Compared to radiation alone. [i] Predicted log cell kill, additional to radiation, from the PK/PD model; other columns are measured values. [j] Data from ref 40. [k] Not significant, $p > 0.05$.

(H_2/Pd anaerobic chamber) conditions in 96-well plates as described previously.[41] The hypoxic cytotoxicity ratio (HCR) was calculated as the intraexperiment ratio aerobic IC_{50}/anoxic IC_{50}; only compounds with HCR > 20 were investigated further.

The relationship between cell killing, drug exposure, and drug metabolism (i.e., the in vitro PK/PD model) was measured as previously described[35,36] by following the clonogenicity of stirred single cell suspensions of HT29 cells for 3 h, at a drug concentration giving approximately one log kill by 1 h, with monitoring of drug concentrations in the extracellular medium by HPLC. This concentration–time data was fitted to determine the apparent first-order rate constant for metabolic consumption, k_{met}.

The in vitro PK/PD model providing the best fit to the clonogenic assay data was determined as previously described,[36] and the CT_{10} (area under the concentration–time curve providing 10% surviving fraction) and M_{10} (amount of BTO metabolized for 10% surviving fraction) were estimated by interpolation. Two models predominated: one in which the log cell kill was proportional to both the drug concentration and to its cumulative bioreductive metabolism (C × M), and one in which log cell kill was proportional to the amount of BTO metabolized (M). For a few compounds, a third model provided a better fit, with log cell kill proportional to the square of the amount of BTO metabolized (M^2). The measured parameter values and best fit PK/PD model are given in Tables 1 and 2, and the associated error estimates are tabulated in the Supporting Information.

Tissue diffusion coefficients, D, of 12 BTOs were measured using HT29 MCLs under 95% O_2 to suppress bioreductive metabolism as previously described.[35] These values, along with previously reported measurements for BTO analogues[36,39] and unpublished data for other BTOs (a total of 73 compounds), were used to develop a multiple regression model to calculate D for the other analogues as described previously.[40] This model extends the reported[39] dependence, for neutral BTOs, of D on logP and MW by replacing logP with the octanol/water distribution coefficient at pH 7.4 (logP$_{7.4}$) and by adding terms for the numbers of hydrogen bond donors and acceptors. The calculated and measured values and the associated error estimates are tabulated in the Supporting Information. The calculated values for all BTOs are shown in Tables 1 and 2. There is a good correlation between the values of D measured in this study and those calculated from the algorithm [using log-transformation: $R^2 = 0.835$, $N = 10$, $p = 0.0002$]. A one-dimensional EVT parameter, the penetration distance into hypoxic tissue assuming planar geometry ($X_{1/2}$), was calculated from the opposing effects of D and k_{met} on tissue transport as previously,[40] providing a ready comparison between analogues: values are given in Tables 1 and 2, and the associated error estimates are tabulated in the Supporting Information.

Spatially Resolved PK/PD Model. The in vivo 3D PK/PD model has been described in detail recently[37,40] Briefly, transport is modeled in the extravascular compartment of a representative tumor microvascular network by solving the Fick's Second Law diffusion-reaction equations using a Green's function method, providing a description of the PK at each point in the tissue region. The transport parameters used in the model are the tissue diffusion coefficient D (estimated in MCLs) and k_{met} for bioreductive drug metabolism under anoxia (scaled to MCL cell density) determined in vitro as above. Using the homogeneous PK/PD model established in vitro for each compound, the log cell kill was predicted at each position in the tumor microregion. The overall cell kill through the whole region was then

calculated for drug only and for drug plus 20 Gy radiation (using the reported radiosensitivity parameters for aerobic and hypoxic HT29 cells).[36] The difference between these gives the model-predicted logs of hypoxic cell kill (LCK$_{pred}$). In addition, the hypoxic cytotoxicity differential (HCD) is calculated as a measure of hypoxic selectivity in the tumor:

$$\text{HCD} = \frac{\text{LCK}_{pred} \text{ in the hypoxic region } (<4 \ \mu\text{M O}_2)}{\text{LCK}_{pred} \text{ in the well oxygenated region } (>30 \ \mu\text{M O}_2)} \quad (1)$$

Compounds were taken forward for evaluation in mice if the model predicted that the plasma AUC required for 1 log kill of the hypoxic subpopulation (AUC$_{pred}$) was less than 20 000 μM·min (i.e., 7-fold higher than for TPZ), with an HCD > 1. Consideration was also given to the solubility of the analogues and identification of a suitable formulation. Thus, BTO **18**, which had poor aqueous solubility, was formulated in a blend of DMSO, PEG, and saline and BTOs **15–17**, **19–21**, **25**, and **26** were not tested in vivo despite passing the in vitro filter. Plasma PK was determined at or near the MTD (below), and the spatially resolved PK/PD model was run again with the measured PK parameters to predict hypoxic LCK at this dose (LCK$_{pred}$). Only those compounds with LCK$_{pred}$ > 0.4 were tested for antitumor activity in vivo.

In Vivo Assays. BTO analogues were formulated as shown in Table 3 as single i.p. doses of BTOs to homozygous nude mice (CD-1 Foxn 1^{nu}). The maximum tolerated dose (MTD) was determined using 1.33-fold dose increments and defined as the highest dose causing no mortality, body weight loss (>15%), or other severe morbidity in any of six mice. Plasma PK of total drug was measured at 75 or 100% of MTD by HPLC and the noncompartmental PK parameters AUC, C_{max} (maximum drug concentration) and $t_{1/2}$ (terminal half-life) were determined. Plasma protein binding was found to be negligible for a series of related BTO analogues;[40] hence, the measured concentrations were therefore assumed to reflect free drug concentrations.

Activity against hypoxic cells in HT29 tumor xenografts was determined by excision assay following treatment of mice with the test drug immediately after a dose of γ radiation (20 Gy) large enough to sterilize the oxic cells in the tumor. Tumors were excised 18 h later, and single cell suspensions prepared and plated to determine the number of surviving clonogens/g of tumor. Surviving fractions (SF) were calculated as the ratio treated/control clonogens/g of tumor, and drug-induced logs of hypoxic cell kill (LCK) was calculated as

$$\log (\text{hypoxic cell kill}) = \log (\text{SF, radiation}) - \log (\text{SF, radiation} + \text{drug}) \quad (2)$$

Results and Discussion

In Vitro Studies. The initial set of neutral BTOs **3–10** with 3-alkyl, 3-alkyloxymethyl, and 3-alkylhydroxyl groups were generally more soluble than TPZ and displayed similar hypoxic cytotoxicity and selectivity (Table 1). The HCR values for 3-phenyl BTO **9** and the 3-methoxy BTO **10** were below the threshold of 20 and were not evaluated further.

The flux of BTO analogues through HT29 MCLs was determined as previously described.[39] In a representative example, the flux of TPZ and BTO **5** was measured through bare Teflon supports (Figure 3A) or through MCLs (Figure 3B). Appearance of **5** in the receiver (distal) compartment of the diffusion chamber was the same as for TPZ using Teflon supports alone, as expected for their similar MW, but was clearly
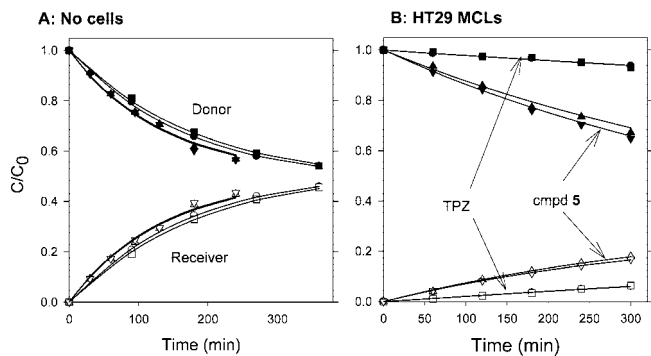

Figure 3. Concentrations of TPZ (circles and squares) and BTO 5 (triangles) as a function of time in the donor (closed symbols) and receiver (open symbols) compartments during a representative flux experiment in the absence of cells, Teflon support membranes alone (A); or with HT29 MCLs (B) under 95% O$_2$ at 37 °C. Concentrations (*C*) were normalized against the initial concentration in the donor compartment (*C*$_0$; 50 μM). The lines are fits to the diffusion model, based on the average thickness of each MCL (148 μm for TPZ and 133 μm for 5) as estimated from the flux of the internal standard urea (not shown).
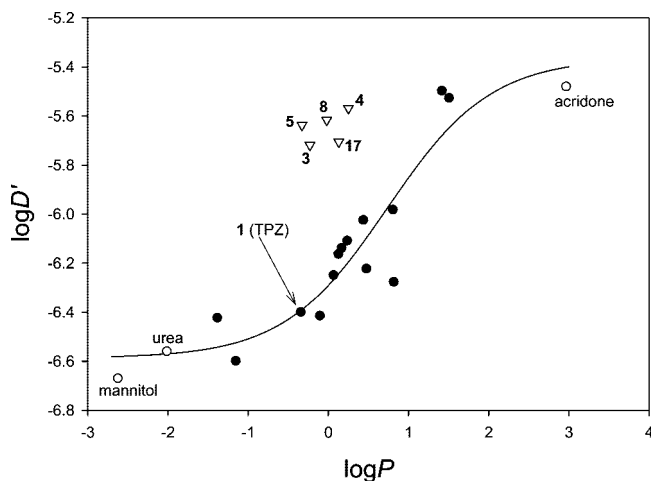

Figure 4. The log *P* dependence of diffusion coefficients of neutral BTOs in HT29 MCLs, (*D'*, corrected to the same M_r as TPZ as described previously; ref 39). Open triangles refer to 3-alkyl compounds lacking hydrogen bond donors. For comparison, values for 3-amino analogues (filled circles) and reference compounds (open circles) are redrawn from ref 39.

faster through MCLs. This faster flux occurred despite some loss of **5** due to metabolism even at this high oxygen concentration (95%), as demonstrated by the greater loss of **5** from the donor than accounted for by its appearance in the receiver compartment (Figure 3B). Fitting the concentration−time curves to a diffusion-reaction model gave an MCL diffusion coefficient, *D*, of (20.89 ± 0.36) × 10^{-7} cm^2 s^{-1}, approximately 5-fold higher than TPZ (measured values of *D* are tabulated in the Supporting Information). The values of *D* are plotted in Figure 4 as a function of logP for the five neutral 3-alkyl BTOs lacking hydrogen-bonding functionality in the side chain for which MCL experiments have been performed. These show higher tissue diffusion coefficients at equivalent logP than the neutral 3-amino BTOs reported previously,[39] which are reproduced in Figure 4. This supports the hypothesis that hydrogen bonding of the 3-NH$_2$ group lowers *D*, accounting for the improved tissue penetration of 3-alkyl analogues at equivalent logP. Consistent with this, the hydroxyl-substituted **6** and **7** also showed low values of *D* relative to their logP values (Supporting Information).

The one electron reduction potentials, $E(1)$, for BTOs **3–7**, and **9** were considerably higher than that of TPZ, reflecting the weaker electron-donating nature of the 3-alkyl ($\sigma_p = -0.17$) or 3-alkyloxy (σ_p ranges from -0.06 to -0.12) substituents compared to the 3-NH_2 substituent ($\sigma_p = -0.66$). This increase in electron affinity for the neutral 3-alkyl BTOs has a strong influence on the rate constant for hypoxic metabolism, k_{met}, (linear regression of $E(1)$ vs log k_{met} gave $r^2 = 0.86$, $P < 0.001$, $n = 8$). These high rates of metabolism compromised gains in EVT due to increased diffusion as reflected by the calculated $X_{1/2}$ values. The exceptions to this, BTOs **4** and **5**, displayed 4-fold increases in k_{met} which were more than compensated for by ca. 6-fold increases in D, resulting in modestly improved $X_{1/2}$ values relative to TPZ.

In an effort to improve aqueous solubility, we added basic tertiary amines to BTOs **11–14**. These provided excellent solubility and the BTOs were more potent under hypoxia than TPZ and had similar hypoxic selectivity. The addition of the polar amine groups lowered D relative to the 3-alkyloxy BTOs **5** and **8**, but the 3-alkylamino BTOs still showed improved diffusion relative to TPZ. The reduction potential of the BTO **13** was found to be ca. 30 mV higher than similar neutral BTOs, presumably as a consequence of the very weak electron-donating effect of the partially charged side chain ($\sigma_p = 0.01$). Hypoxic metabolism was further increased, by up to 11-fold relative to TPZ, for the alkylamino BTOs **11–14**, completely outweighing the modest improvements in D and compromising the EVT of these basic BTO analogues.

Our previous studies[40,41] demonstrated the ability of electron-donating substituents on the benzo ring of BTO analogues to lower $E(1)$ values and hypoxic metabolism. The neutral 6-alkyl or 6-alkyloxy BTOs with 3-ethyl or 3-ethyloxy substituents **15–21** displayed increased lipophilicity, which was moderated by the presence of free hydroxyl groups (**16**, **19**, **21**) (Table 2). Aqueous solubility for **15–21** was low with the exception of the 6-hydroxyethyloxy BTO **19**. The 6-methyl BTOs **15–17** had similar hypoxic potency and selectivity in HT29 cells to TPZ, with improved selectivity observed in SiHa cells, while the 6-alkoxy BTOs **18–21** were less potent and had similar hypoxic selectivity to TPZ. The increased lipophilicity of **15–21** translates to increased diffusion, with the presence of a free hydroxyl hydrogen-bond donor strongly impairing diffusion (**16**, **19**, **21**). The increased electron donation from the 6-substituents is confirmed by the lowered $E(1)$ values for **15** and **18**, -418 and -472 mV, respectively. This has a clear impact on the rates of hypoxic metabolism with 6-methyl BTOs **15–17** having slightly raised k_{met} values, and 6-alkoxy BTOs **18–21** having lightly lower k_{met} values, relative to TPZ. The reduced rate of hypoxic metabolism, combined with increases in D, gave up to 3-fold increases in $X_{1/2}$, signaling significantly improved EVT.

The poor solubility of the neutral BTOs **15–21**, coupled with the lower in vivo potency predicted for the alkoxy BTOs **19–21** (vide infra), led us to attach solubilizing amine side chains via 6-alkoxy substituents on the benzo ring, BTOs **22–24**, with the expectation that the electron-withdrawing tertiary amine would both provide solubility and moderate the electronic effect of the alkoxy substituent. We also explored neutral and basic side chains attached at the 7-position, BTOs **25–28**. The 7-alkoxy substituents are expected to have a smaller electronic influence, lowering $E(1)$ by ca. 40 mV, whereas the 6-alkoxy substituents lower $E(1)$ by ca. 100 mV.[41] The presence of the basic side chains on BTOs **22–24** provided excellent solubility and increased hypoxic potency relative to the corresponding neutral BTOs **19–21**, with the near neutral morpholide **22** having

intermediate potency, while all displayed excellent hypoxic selectivity. The presence of the lipophilic amine group provided increased diffusion relative to the corresponding hydroxy analogues (e.g., compare **22** with neutral **21**, and **23**, **24** with neutral **19**), emphasizing the negative influence of hydrogen-bond donors on diffusion. The morpholide **22** had a similar k_{met} to TPZ resulting in overall improved EVT ($X_{1/2} = 64\ \mu m$) relative to TPZ, whereas increases in k_{met} seen with the stronger bases (**23**, **24**) offset potential gains in EVT due to increased D. A similar pattern to that seen for **20–23** was observed in the 7-alkoxy BTOs **25–28**. The neutral BTOs **25** and **26** displayed low solubility, which was increased by the addition of basic side chains for BTOs **27** and **28**. The hypoxic potencies of the 7-substituted BTOs (**25–28**) were consistently greater than the corresponding 6-substituted BTOs **20–23** in accord with the higher $E(1)$ value observed for **27** compared to **22**, while all displayed good hypoxic selectivity. Diffusion coefficients for **25–28** followed the same pattern as for **20–23**, but were lower, whereas k_{met} values for **25–28** were consistently higher than the corresponding values for **20–23**. This resulted in lower EVT for **25–28** than for the 6-substituted analogues **20–23**.

Modeling. The in vitro PK/PD model parameters, combined with the estimates of EVT properties, were used in the spatially resolved PK/PD model to calculate AUC_{pred} (the area under the plasma concentration-time curve required to give 1 log of cell kill of hypoxic cells in HT29 tumors), and HCD (the predicted hypoxic cytotoxicity differential in these tumors) for **3–8**. We have previously shown[40] that TPZ has a modest AUC requirement of 10 300 $\mu M \cdot min$ and its calculated hypoxic selectivity is consistent with its observed in vivo activity.[36,37] For the compounds of Table 1, only BTOs **4** and **5** had reasonable AUC_{pred} values ($<20\ 000\ \mu M \cdot min$) with an HCD significantly greater than 1 and were advanced to in vivo evaluation. AUC_{pred} values were slightly lower than TPZ for the 6-methyl BTOs **15–17** and 6-methoxy BTO **18**, and slightly higher for the alkoxy BTOs **19–21**, reflecting their lower potency. Increased HCD values relative to TPZ were calculated for **15–21**, with the largest increase in selectivity expected for the 6-alkoxy BTOs **18–21**. The hypoxic potency of **22–28** was reflected in lower AUC_{pred}, while increased in vivo selectivity was predicted for all but **23** and **28**.

In Vivo Studies. Application of the in vivo filters of AUC_{pred} ($<20\ 000\ \mu M \cdot min$) and HCD ($>1$) (Figure 2) eliminated all the unsubstituted 3-alkyl BTOs except for **4** and **5**. All of the 6- and 7-substituted BTOs passed the initial thresholds; however, difficulties with formulation of the neutral BTOs, such as **18**, meant that neutral BTOs with low aqueous solubility and/or lower hypoxic potency (**15–17**, **19–21**, **25**, and **26**) were not advanced to in vivo testing. Thus, three neutral 3-alkyl BTOs (**4**, **5**, and **18**) and four soluble BTOs (**22–24** and **27**) were tested in vivo.

The 3-alkyl BTOs were generally less toxic in vivo than TPZ, with the exception of **24**. Determination of plasma PK allowed calculation of LCK_{pred} in combination with radiation and BTOs with $LCK_{pred} > 0.4$ were evaluated in the tumor excision assay. BTO **18**, although having exceptional EVT, gave a relatively low C_{max} of 72 μM, which compromised its LCK_{pred} (Table 3). BTO **24** displayed a very low AUC and C_{max}, and the PK/PD model predicted little hypoxic cell killing in addition to radiation and was not evaluated further.

Generally, the BTOs showed little single agent activity, in keeping with the proposed mechanism of action. We have previously shown[40] that TPZ, given at 133 $\mu mol\ kg^{-1}$ (75% of MTD), gave a LCK of 0.59 logs and that **2** when administered
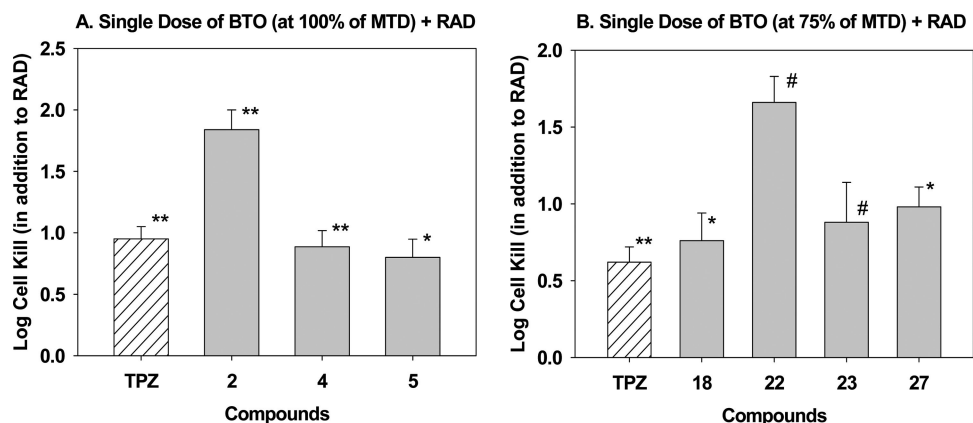
Figure 5. In vivo activity of BTOs against hypoxic cells in HT29 human tumor xenografts following a single i.p. dose 5 min after irradiation (RAD, 20 Gy). Hypoxic cell killing was determined as [log(clonogens/g of tumor for RAD only)] − [log(clonogens/g of tumor for RAD + drug)]. P values vs RAD: *$P < 0.05$, **$P < 0.01$, #$P < 0.001$. A, BTO given at 100% of MTD 5 min. B, BTO given at 75% of MTD.

at 1000 μmol kg^{-1} (100% of MTD) had ca. 3-fold higher activity (LCK, 1.84 ± 0.16) than TPZ against hypoxic cells in HT29 tumors (Figure 5 and Table 3). The activity of the neutral BTOs **4** and **5** seen previously in the fractionated irradiation experiments with murine SCCVII tumors[42] was confirmed as a single dose in the HT29 model with LCK values of 0.89 and 0.80, respectively. The neutral BTO **18** had similar activity to **4** and **5**, although it was given at 75% of the MTD. The three soluble BTO analogues tested, **22**, **23**, and **27**, displayed significant hypoxic cell killing in addition to radiation with **22** ca. 3-fold more active than TPZ. BTO **22** is currently being tested further in combination with radiation against multiple human tumor xenografts, both as a single dose and in a fractionated regimen.

Conclusions

We have explored the effect of hydrogen-bond donors on EVT in this class of 3-alkyl BTOs. Replacement of the 3-NH$_2$ of TPZ with small alkyl substituents provided modest increases in aqueous solubility and increased diffusion sufficiently to offset increases in hypoxic metabolism due to raised electron affinity. The addition of hydrogen-bond donors such as hydroxyl groups severely impaired diffusion while polar amine groups increased solubility, but decreased diffusion and increased hypoxic metabolism, thus compromising EVT. Only two BTOs of the initial set, **4** and **5**, were predicted to be active in vivo, and this was confirmed in the tumor excision assay.

The addition of lipophilic electron-donating 6-substituents increased diffusion and lowered hypoxic metabolism, contributing to excellent EVT. The positive effect was reduced by the addition of hydrogen-bond donors and acceptors. The low solubility of these neutral BTO analogues **18–21** precluded in vivo testing of all but **18**. BTO **18** was found to be active in vivo with a relatively low C_{max} compromising activity. The addition of solubilizing amine groups via a 6-alkoxy linker (BTOs **22–24**) provided increased aqueous solubility, but had a modest negative impact on EVT through lowered diffusion relative to the neutral analogues **19–21**. A similar pattern of activity was seen with 7-substituted BTOs **25–28**, although hypoxic potency and metabolism was consistently higher and the diffusion and EVT consistently lower than the corresponding 6-substituted analogues. Model predictions of activity for the soluble BTOs **22**, **23**, and **27** were confirmed with all three more active in vivo than TPZ at equitoxic doses.

PK/PD-guided screening of BTOs designed to have improved EVT has assisted us to identify four novel BTO analogues with

activity against hypoxic tumor cells in vivo. The advantages of these compounds are illustrated by the morpholide **22** in which replacement of the 3-amino group of TPZ with a 3-ethyl provides a higher tissue diffusion coefficient, reflecting the importance of minimizing hydrogen-bond donor functionality in designing bioreductive prodrugs able to reach their target cells. The resulting increase in one-electron reduction potential, and thus bioreductive metabolism, would preclude efficient penetration into hypoxic tissue, but is compensated by an electron-donating 6-alkoxy side chain bearing a weakly basic morpholino side chain that increases aqueous solubility with little impact on lipophilicity at neutral pH. Reflecting these improvements, the lead compound **22** displayed ca. 3-fold greater log cell kill of hypoxic cells in HT29 tumors than TPZ and is the subject of ongoing evaluation.

Experimental Section

Chemistry. General experimental details are described in the Supporting Information. TPZ and BTO **2** were synthesized as previously described.[40]

Example of Synthetic Methods. (See Supporting Information for full experimental details of compounds **3–28**.)

Preparation of 1-Oxides. General Method A. Pd(PPh$_3$)$_4$ (0.1 mmol) was added to a stirred, degassed solution of chloride (2.0 mmol) and stannane (2.4 mmol) in DME (20 mL), and the solution was stirred under N$_2$ at reflux temperature for 16 h. The solvent was evaporated, and the residue was dissolved in DCM (10 mL) and stirred with saturated aqueous KF solution (10 mL) for 30 min. The mixture was filtered through Celite, the Celite was washed with DCM, and the combined organic filtrate washed with water. The organic fraction was dried, the solvent was evaporated, and the residue was purified by chromatography, eluting with DCM to give product, which was, if necessary, further purified by chromatography, eluting with 20% EtOAc/pet. ether, to give the 3-alkyl-BTO.

Preparation of 1,4-Dioxides. General Method B. Hydrogen peroxide (70%, 10 mmol) was added dropwise to a stirred solution of trifluoroacetic anhydride (10 mmol) in DCM (20 mL) at 0 °C. The mixture was stirred at 0 °C for 5 min, warmed to 20 °C, stirred for 10 min, and cooled to 5 °C. The mixture was added to a stirred solution of 1-oxide (1.0 mmol) [and TFA (5.0 mmol) for substrates with an amine side chain] in DCM (15 mL) at 0 °C, and the mixture was stirred at 20 °C for 6–16 h. The solution was carefully diluted with water (20 mL), the mixture was made basic with aqueous NH$_4$OH solution, and the mixture was stirred for 15 min and then extracted with CHCl$_3$ (5 × 50 mL). The organic fraction was dried, and the solvent was evaporated. The residue was purified by chromatography, eluting with a gradient (0–15%) of MeOH/DCM, to give the 1,4-dioxide.

Preparation of 1-Oxides. General Method C. MsCl (5.0 mmol) was added to a stirred solution of alcohol (4.0 mmol) and Et$_3$N (5.2 mmol) in dry DCM (50 mL) at 20 °C, and the solution was stirred for 2 h. The solution was diluted with DCM (50 mL) and washed with water (2 × 30 mL), brine (50 mL), and the organic fraction was dried and the solvent was evaporated. The residue was dissolved in THF (50 mL) and amine (100 mmol) added, and the solution was heated at reflux temperature for 6 h, then stirred at 20 °C for 16 h. The solvent was evaporated and the residue was partitioned between EtOAc (100 mL) and water (100 mL). The aqueous fraction was extracted with EtOAc (3 × 50 mL), the combined organic fraction was dried, and the solvent was evaporated. The residue was purified by chromatography, eluting with a gradient (0–10%) of MeOH/EtOAc, to give 1-oxide.

Preparation of 1-Oxides. General Method D. Sodium hydride (2.0 mmol) was added to a stirred suspension of fluoride (1.6 mmol) in alcohol (10 mL), and the resulting solution was stirred at 20 °C for 3 h under N$_2$. The solvent was evaporated, and the residue was partitioned between DCM (30 mL) and water (30 mL). The organic fraction was dried, and the solvent was evaporated. The residue was purified by column chromatography, eluting with a gradient (0–5%) of MeOH/DCM, to give the 1-oxide.

Supporting Information Available: Experimental details and characterization data for synthetic intermediates and BTOs **3–28**; experimental details for the physicochemical and biological methods; tables of physicochemical and in vitro data with estimates of errors. This information is available free of charge via the Internet at http://pubs.acs.org.

References

(1) Evans, S. M.; Koch, C. J. Prognostic significance of tumor oxygenation in humans. *Cancer Lett.* **2003**, *195*, 1–16, and references therein.

(2) Harris, A. L. Hypoxia-a key regulatory factor in tumour growth. *Nat. Rev. Cancer* **2002**, *2*, 38–47.

(3) Semenza, G. L. HIF-1 and tumor progression: pathophysiology and therapeutics. *Trends Mol. Med.* **2002**, *8*, S62–S67.

(4) Pennachietti, S.; Michieli, P.; Galluzzo, M.; Mazzone, M.; Giordano, S.; Comoglio, P. M. Hypoxia promotes invasive growth by transcriptional activation of the met protooncogene. *Cancer Cell* **2003**, *3*, 347–361.

(5) Cairns, R. A.; Hill, R. P. Acute hypoxia enhances spontaneous lymph node metastasis in an orthotopic murine model of human cervical carcinoma. *Cancer Res.* **2004**, *64*, 2054–2061.

(6) Subarsky, P.; Hill, R. P. The hypoxic tumour microenvironment and metastatic progression. *Clin. Exp. Metastases* **2003**, *20*, 237–250.

(7) Durand, R. E. The influence of microenvironmental factors during cancer therapy. *In Vivo* **1994**, *8*, 691–702.

(8) Tannock, I. F. Conventional cancer therapy: promise broken or promise delayed. *Lancet* **1998**, *351* (Suppl 2), 9–16.

(9) Brown, J. M.; Wilson, W. R. Exploiting tumor hypoxia in cancer treatment. *Nat. Rev. Cancer* **2004**, *4*, 437–447.

(10) Nordsmark, M.; Overgaard, M.; Overgaard, J. Pretreatment oxygenation predicts radiation response in advanced squamous cell carcinoma of the head and neck. *Radiother. Oncol.* **1996**, *41*, 31–39.

(11) Fyles, A. W.; Milosevic, M.; Wong, R.; Kavanagh, M. C.; Pintilie, M.; Sun, A.; Chapman, W.; Levin, W.; Manchul, L.; Keane, T. J.; Hill, R. P. Oxygenation predicts radiation response and survival in patients with cervix cancer. *Radiother. Oncol.* **1998**, *48*, 149–156.

(12) Koukourakis, M. I.; Bentzen, S. M.; Giatromanolaki, A.; Wilson, G. D.; Daley, F. M.; Saunders, M. I.; Dische, S.; Sivridis, E.; Harris, A. L. Endogenous markers of two separate hypoxia response pathways (hypoxia inducible factor 2 alpha and carbonic anhydrase 9) are associated with radiotherapy failure in head and neck cancer patients recruited in the CHART randomized trial. *J. Clin. Oncol.* **2006**, *24*, 727–735.

(13) Denny, W. A.; Wilson, W. R.; Hay, M. P. Recent developments in the design of bioreductive drugs. *Br. J. Cancer* **1996**, *74*, S32–S38.

(14) Brown, J. M.; Giaccia, A. J. The unique physiology of solid tumors: opportunities (and problems) for cancer therapy. *Cancer Res.* **1998**, *58*, 1408–1416.

(15) Brown, J. M. SR 4233 (tirapazamine): a new anticancer drug exploiting hypoxia in solid tumours. *Br. J. Cancer* **1993**, *67*, 1163–1170.

(16) Denny, W. A.; Wilson, W. R. Tirapazamine: a bioreductive anticancer drug that exploits tumour hypoxia. *Expert Opin. Invest. Drugs* **2000**, *9*, 2889–2901.

(17) Patterson, A. V.; Saunders, M. P.; Chinje, E. C.; Patterson, L. H.; Stratford, I. J. Enzymology of tirapazamine metabolism: a review. *Anti-Cancer Drug Des.* **1998**, *13*, 541–573.

(18) Anderson, R. F.; Shinde, S. S.; Hay, M. P.; Gamage, S. A.; Denny, W. A. Activation of 3-amino-1,2,4-benzotriazine 1,4-dioxide antitumor agents to oxidizing species following their one-electron reduction. *J. Am. Chem. Soc.* **2003**, *125*, 748–756.

(19) Shinde, S. S.; Anderson, R. F.; Hay, M. P.; Gamage, S. A.; Denny, W. A. Oxidation of 2-deoxyribose by benzotriazinyl radicals of antitumor 3-amino-1,2,4-benzotriazine 1,4-dioxides. *J. Am. Chem. Soc.* **2004**, *126*, 7853–7864.

(20) Wang, J.; Biedermann, K. A.; Brown, J. M. Repair of DNA and chromosome breaks in cells exposed to SR 4233 under hypoxia or to ionizing radiation. *Cancer Res.* **1992**, *52*, 4473–4477.

(21) Siim, B. G.; van Zijl, P. L.; Brown, J. M. Tirapazamine-induced DNA damage measured using the comet assay correlates with cytotoxicity towards hypoxic tumour cells in vitro. *Br. J. Cancer* **1996**, *73*, 952–960.

(22) Siim, B. G.; Menke, D. R.; Dorie, M. J.; Brown, J. M. Tirapazamine-induced cytotoxicity and DNA damage in transplanted tumors: relationship to tumor hypoxia. *Cancer Res.* **1997**, *57*, 2922–2928.

(23) Siim, B. G.; Pruijn, F. B.; Sturman, J. R.; Hogg, A.; Hay, M. P.; Brown, J. M.; Wilson, W. R. Selective potentiation of the hypoxic cytotoxicity of tirapazamine by its 1-*N*-oxide metabolite SR 4317. *Cancer Res.* **2004**, *64*, 736–742.

(24) Brown, J. M; Wang, L. H. Tirapazamine: laboratory data relevant to clinical activity. *Anti-Cancer Drug Des.* **1998**, *13*, 529–539.

(25) Marcu, L.; Olver, I. Tirapazamine: From bench to clinical trials. *Curr. Clin. Pharmacol.* **2006**, *1*, 71–79.

(26) Doherty, N.; Hancock, S. L.; Kaye, S.; Coleman, C. N.; Shulman, L.; Marquez, C.; Mariscal, C.; Rampling, R.; Senan, S.; Roemeling, R. V. Muscle cramping in phase I clinical trials of tirapazamine (SR 4233) with and without radiation. *Int. J. Radiat. Oncol. Biol. Phys.* **1994**, *29*, 379–382.

(27) Rishin, D.; Peters, L.; Hicks, R.; Hughes, P.; Fisher, R.; Hart, R.; Sexton, M.; D'Costa, I.; von Roemeling, R. Phase I trial of concurrent tirapazamine, cisplatin, and radiotherapy in patients with advanced head and neck cancer. *J. Clin. Oncol.* **2001**, *19*, 535–542.

(28) Rischin, D.; Peters, L.; Fisher, R.; Macann, A.; Denham, J.; Poulsen, M.; Jackson, M.; Kenny, L.; Penniment, M.; Corry, J.; Lamb, D.; McClure, B. Tirapazamine, cisplatin, and radiation versus fluorouracil, cisplatin, and radiation in patients with locally advanced head and neck cancer: a randomized phase II trial of the Trans-Tasman Radiation Oncology Group (TROG 98.02). *J. Clin. Oncol.* **2005**, *23*, 79–87.

(29) Le, Q.-T.; Taira, A.; Budenz, S.; Dorie, M. J.; Goffinet, D. R.; Fee, W. E.; Goode, R.; Bloch, D.; Koong, A.; Brown, J. M.; Pinto, H. A. Mature results from a randomized phase II trial of cisplatin plus 5-fluouracil and radiotherapy with or without tirapazamine in patients with respectable stage IV head and neck squamous cell carcinomas. *Cancer* **2006**, *106*, 1940–1949.

(30) Durand, R. E.; Olive, P. L. Physiologic and cytotoxic effects of tirapazamine in tumor-bearing mice. *Radiat. Oncol. Invest.* **1997**, *5*, 213–219.

(31) Durand, R. E.; Olive, P. L. Evaluation of bioreductive drugs in multicell spheroids. *Int. J. Radiat. Oncol. Biol. Phys.* **1992**, *22*, 689–692.

(32) Hicks, K. O.; Fleming, Y.; Siim, B. G.; Koch, C. J.; Wilson, W. R. Extravascular diffusion of tirapazamine: effect of metabolic consumption assessed using the multicellular layer model. *Int. J. Radiat. Oncol. Biol. Phys.* **1998**, *42*, 641–649.

(33) Kyle, A. H.; Minchinton, A. I. Measurement of delivery and metabolism of tirapazamine to tumour tissue using the multilayered cell culture model. *Cancer Chemother. Pharmacol.* **1999**, *43*, 213–220.

(34) Baguley, B. C.; Hicks, K. O.; Wilson, W. R. Tumour cell cultures in drug development. In *Anticancer Drug Development*; Baguley, B. C., Kerr, D. J., Eds.; Academic Press: San Diego, 2002; pp 269–284.

(35) Hicks, K. O.; Pruijn, F. B.; Sturman, J. R.; Denny, W. A.; Wilson, W. R. Multicellular resistance to tirapazamine is due to restricted extravascular transport: a pharmacokinetic/ pharmacodynamic study in multicellular layers. *Cancer Res.* **2003**, *63*, 5970–5977.

(36) Hicks, K. O.; Siim, B. G.; Pruijn, F. B.; Wilson, W. R. Oxygen dependence of the metabolic activation and cytotoxicity of tirapazamine: implications for extravascular transport and activity in tumors. *Radiat. Res.* **2004**, *161*, 656–666.

(37) Hicks, K. O.; Pruijn, F. B.; Secomb, T. W.; Hay, M. P.; Hsu, R.; Brown, J. M.; Denny, W. A.; Dewhirst, M. W.; Wilson, W. R. Use of three-dimensional tissue cultures to model extravascular transport and predict in vivo activity of hypoxia-targeted anticancer drugs. *J. Natl. Cancer Inst.* **2006**, *98*, 1118–1128.

(38) Hicks, K. O.; Myint, H.; Patterson, A. V.; Pruijn, F. B.; Siim, B. G.; Patel, K.; Wilson, W. R. Oxygen dependence and extravascular transport of hypoxia-activated prodrugs: comparison of the dinitrobenzamide mustard PR-104A and tirapazamine. *Int. J. Radiat. Oncol. Biol. Phys.* **2007**, *69*, 560–571.

(39) Pruijn, F. B.; Sturman, J.; Liyanage, S.; Hicks, K. O.; Hay, M. P.; Wilson, W. R. Extravascular transport of drugs in tumor tissue: Effect of lipophilicity on diffusion of tirapazamine analogues in multicellular layer cultures. *J. Med. Chem.* **2005**, *48*, 1079–1087.

(40) Hay, M. P.; Hicks, K. O.; Pruijn, F. B.; Pchalek, K.; Siim, B. G.; Wilson, W. R.; Denny, W. A. Pharmacokinetic/pharmacodynamic model-guided identification of hypoxia-selective 1,2,4-benzotriazine 1,4-dioxides with antitumor activity: the role of extravascular transport. *J. Med. Chem.* [Online early access]. DOI: 10.1021/jm070670g.

Published online: November 15, 2007. http://pubs.acs.org/cgi-bin/asap.cgi/jmcmar/asap/html/jm070670g.html.

(41) Hay, M. P.; Gamage, S. A.; Kovacs, M. S.; Pruijn, F. B.; Anderson, R. F.; Patterson, A. V.; Wilson, W. R.; Brown, J. M.; Denny, W. A. Structure-activity relationships of 1,2,4-benzotriazine 1,4-dioxides as hypoxia-selective analogues of tirapazamine. *J. Med. Chem.* **2003**, *46*, 169–182.

(42) Kelson, A. B.; McNamara, J. P.; Pandey, A.; Ryan, K. J.; Dorie, M. J.; McAfee, P. A.; Menke, D. R.; Brown, J. M.; Tracy, M. 1,2,4-Benzotriazine 1,4-dioxides. An important class of hypoxic cytotoxins with antitumor activity. *Anti-Cancer Drug Des.* **1998**, *13*, 575–592.

(43) Hay, M. P.; Denny, W. A. A new and versatile synthesis of 3-alkyl-1,2,4-benzotriazine-1,4-dioxides: preparation of the bioreductive cytotoxins SR4895 and SR4941. *Tetrahedron Lett.* **2002**, *43*, 9569–9571.

(44) Pchalek, K.; Hay, M. P. Stille coupling reactions in the synthesis of hypoxia-selective 3-alkyl-1,2,4-benzotriazine 1,4-dioxide anticancer agents. *J. Org. Chem.* **2006**, *71*, 6530–6535.

(45) Siim, B. G.; Hicks, K. O.; Pullen, S. M.; van Zijl, P. L.; Denny, W. A.; Wilson, W. R. Comparison of aromatic and tertiary amine N-oxides of acridine DNA intercalators as bioreductive drugs - cytotoxicity, DNA binding, cellular uptake, and metabolism. *Biochem. Pharmacol.* **2000**, *60*, 969–978.

(46) Patel, K. B.; Willson, R. L. Semiquinone free radicals and oxygen. Pulse radiolysis study of one electron equilibria. *J. Chem. Soc. Faraday Trans.* **1973**, *69*, 814–819.

JM701037W